Article

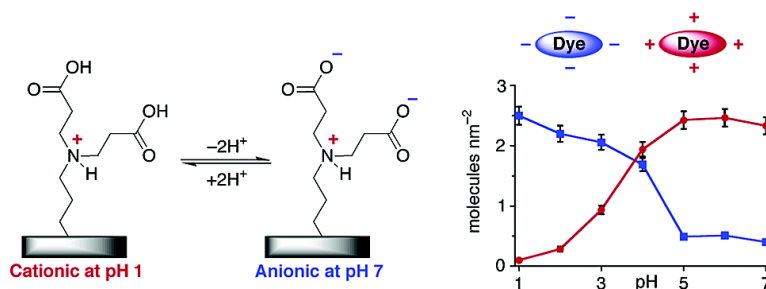# Surfaces Designed for Charge Reversal

James R. Matthews, Dns Tuncel, Robert M. J. Jacobs, Colin D. Bain, and Harry L. Anderson

More About This Article

Additional resources and features associated with this article are available within the HTML version:

- Supporting Information
- Links to the 3 articles that cite this article, as of the time of this article download
- Access to high resolution figures
- Links to articles and content related to this article
- Copyright permission to reproduce figures and/or text from this article

View the Full Text HTML

Surfaces Designed for Charge Reversal

James R. Matthews, Dönüs Tuncel, Robert M. J. Jacobs, Colin D. Bain, and
Harry L. Anderson*

*Contribution from the Department of Chemistry, University of Oxford,
South Parks Road, Oxford, OX1 3QY, U.K.*

Received August 29, 2002; E-mail: harry.anderson@chemistry.ox.ac.uk

Abstract: We have created surfaces which switch from cationic at pH < 3 to anionic at pH > 5, by attaching aminodicarboxylic acid units to silica and gold substrates. Charge reversal was demonstrated by monitoring the adsorption of cationic dyes (methylene blue and a tetracationic porphyrin) and an anionic sulfonated porphyrin, at a range of pH using UV−vis absorption and reflection spectroscopy. The cationic dyes bind under neutral conditions (pH 5−7) and are released at pH 1−4, whereas the anionic dye binds under acidic conditions (pH 1−4) and is released at pH 5−7. Gold surfaces were functionalized with two different amphoteric disulfides with short $(CH_2)_2$ and long $(CH_2)_{10}CONH(CH_2)_6$ linkers; the longer disulfide gave surfaces exhibiting charge reversal in a narrower pH range. Adsorption is much faster on the functionalized gold ($t_{1/2} = 62$ s) than on functionalized silica ($t_{1/2} = 6900$ s), but the final extents of coverage on both surface are similar, for a given dye at a given pH, with maximal coverages of around 2 molecules nm^{-2}. These charge-reversal processes are reversible and can be repeatedly cycled by changing the pH. We have also created surfaces which undergo irreversible proton-triggered charge switching, using a carbamate-linked thiol carboxylic acid which cleaves in acid. These surfaces are versatile new tools for controlling electrostatic self-assembly at surfaces.

Introduction

The electrostatic assembly of molecules, nanoparticles, and even viruses on charged surfaces is becoming a widely used technique.[1] The ability to switch this interaction on and off, between attraction and repulsion, will have important applications in diverse fields ranging from material science to microbiology. Here we present the first examples of surfaces designed for controlled charge reversal.[2] We have created surfaces which switch reversibly from cationic to anionic in a narrow pH range and other surfaces which undergo irreversible proton-triggered charge switching. These functional surfaces were created using both silane−silica and thiol−gold chemistry.[3,4] Charge reversal was demonstrated by monitoring the adsorption of anionic and cationic chromophores (**1**−**3**). Charge-reversible surfaces are versatile control elements for the binding, manipulation, and release of charged guests.
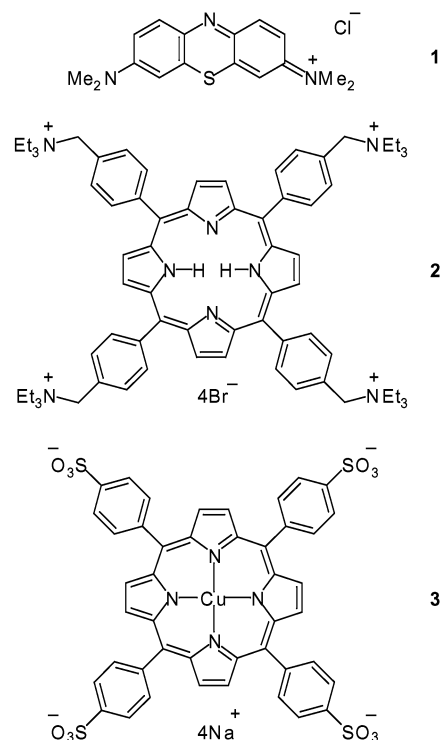
(1) Mrksich, M. *Chem. Soc. Rev.* **2000**, *29*, 267−273. Shipway, A. N.; Katz, E.; Willner, I. *ChemPhysChem* **2000**, *1*, 18−52. Britt, D. W.; Buijs, J.; Hlady, V. *Thin Solid Films* **1998**, *327−329*, 824−828.

(2) Many naturally occurring surfaces, such as proteins and metal oxides, are amphoteric and undergo charge reversal over a wide pH range, due to protonation in acid and deprotonation or coordination of hydroxide. However these surfaces are not suitable for use as control elements in self-assembly because very large changes in pH are required to achieve charge reversal and because they are difficult to fabricate. The design of surfaces capable of switching hydrophobicity in response to changes in electrical potential was reported recently: Lahann, J.; Mitragotri, S.; Tran, T.-N.; Kaido, H.; Sundaram, J.; Choi, I. S.; Hoffer, S.; Somorjai, G. A.; Langer, R. *Science* **2003**, *299*, 371−374.

(3) Ulman, A. *An introduction to ultrathin organic films: from Langmuir−Blodgett to self-assembly*; Academic Press: Boston, 1991. Ulman, A. *Chem. Rev.* **1996**, *96*, 1533−1554.

(4) Nuzzo, R. G.; Fusco, F. A.; Allara, D. L. *J. Am. Chem. Soc.* **1987**, *109*, 2358−2368. Bain, C. D.; Whitesides, G. M. *Adv. Mater.* **1989**, *1*, 506−512.

Results and Discussion

Design. Several ways of switching the charge on a surface can be envisaged, such as (a) electrochemical oxidation and reduction, (b) cation or anion coordination, (c) protonation, and

**Scheme 1.** Synthesis of a Charge-Reversible Silica Surface[a]
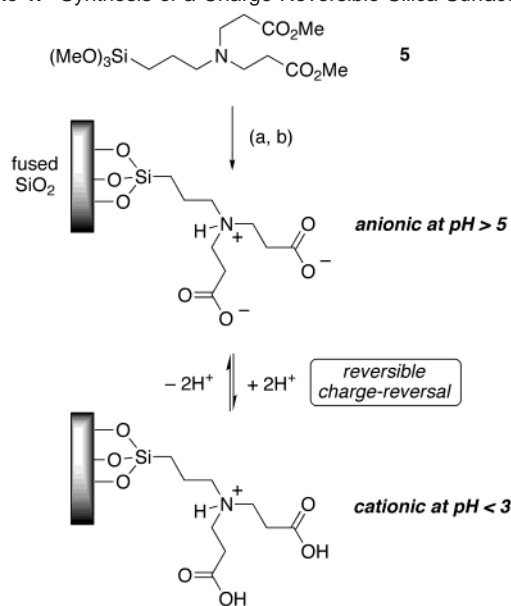
(d) covalent modification. We chose to focus on the last two of these options. Proton transfer is fast, reversible, easy to monitor, and easy to drive by pH. We set out to design surfaces exhibiting charge reversal in response to small pH changes. Many molecules undergo charge reversal over a wide pH range, for example, natural α-amino acids are cationic below pH 3 (when the amine and carboxylic acid are both protonated) but require pH > 10 to fully deprotonate the nitrogen, leaving a wide pH gap in which the molecule is weakly charged. This pH gap is minimized by using two equivalent protonation sites, as for example in *N*-propyl-3,3′-iminodipropionic acid, **4**. At low pH both carboxylic acids and the amine are protonated giving a single positive charge. The pH need only be raised high enough to deprotonate the carboxylic acids ($pK_a \approx 3.5$) for the net charge to reverse from +1 to −1.
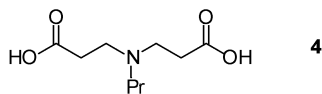

We decided to make charge-reversible surfaces by grafting amino acid **4** to silica and gold surfaces.[5] In both cases this amphoteric unit was coupled to the surface via the central nitrogen, by replacing the *n*-propyl group with a suitable linker. Silica surfaces were functionalized with the trimethoxysilane **5** (Scheme 1). We chose to use the methyl ester **5**, which requires hydrolysis on the surfaces, rather than the free carboxylic acid, because this acid was found to be unstable. Gold was functionalized with two different amphoteric disulfides, **6** and **7**, with short $(CH_2)_2$ and long $(CH_2)_{10}CONH(CH_2)_6$ linkers. The short

(5) The stability of the silane−silica linkage under the conditions of our dye adsorption experiments (pH 1−7 water) was verified by testing fused silica functionalization with methyl orange. 4-Dimethylaminoazobenzene-4′-sulfonyl chloride was reacted with (aminopropyl)trimethoxysilane in toluene and then used directly to functionalize fused silica. These surfaces were immersed in water over the pH range 1−7 over a period of 14 days. UV−vis spectra were acquired to confirm that the dye, with an approximate coverage of 2.0 molecules nm^{-2}, remained attached to the surface.

Scheme 2. Synthesis of an Irreversible Proton-Triggered Charge-Switching Surface[a]
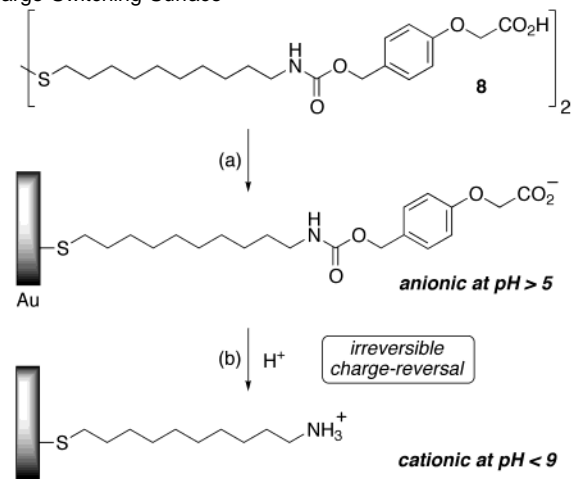
disulfide is more readily accessible, but the longer disulfide was expected to form more stable monolayers due to van der Waals interaction between the long aliphatic chains and hydrogen-bonding between the amides.[6]
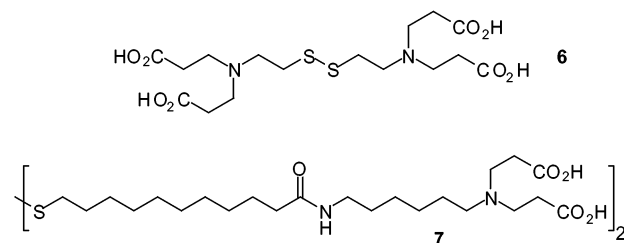
Irreversible proton-triggered charge-switching surfaces were designed using a carbamate-linked disulfide carboxylic acid **8**, which can be cleaved at low pH to unmask ammonium functionality as shown in Scheme 2. This type of acid-labile linker is widely used in solid-phase synthesis.[7]

Synthesis. Detailed schemes and experimental procedures for the synthesis of compounds **5**−**8** are provided in Supporting Information. Trimethoxysilane **5** was prepared in 92% yield by treatment of (aminopropyl)trimethoxysilane with methyl acrylate. Disulfide **6** was prepared by reacting cystamine with *tert*-butyl acrylate, followed by cleavage of the *tert*-butyl esters with TFA. Similar chemistry was used to prepare **7** in four steps from 1,6-diaminohexane. The key step in the synthesis of carbamate **8** was coupling of a disulfide isocyanate (generated in situ by Curtis rearrangement) with a benzyl alcohol.

Fused silica microscope slides were functionalized by immersion in a solution of trimethoxysilyl derivative **5**, followed by hydrolysis in aqueous imidazole[8,9] (Scheme 1). Monitoring by attenuated total reflection infrared (ATR-IR) confirmed that these conditions hydrolyze the surface-bound methyl esters,

(6) Sabapathy, R. C.; Bhattacharyya, S.; Leavy, M. C.; Cleland, W. E.; Hussey, C. L. *Langmuir* **1998**, *14*, 124−136.

(7) Eggenweiler, H.-M. *Drug Discovery Today* **1998**, *3*, 552−560. Wang, S.-S. *J. Am. Chem. Soc.* **1973**, *95*, 1328−1333.

(8) Menegheli, P.; Farah, J. P. S.; El Seoud, O. A. *Ber. Bunsen-Ges. Phys. Chem.* **1991**, *95*, 1610−1615.

(9) As a control experiment, we investigated the hydrolysis of 3,3′-imino-dipropionic acid dimethyl ester, in 2.6 M imidazole in D_2O by ^{1}H NMR.; this reaction reaches completion in 7 days at 20 °C.

without removing the silane, as discussed below. Harsher hydrolysis conditions were avoided so as not cleave the silane from the surface.

Monolayers of **6**−**8** were assembled on gold from solutions in water or DMSO.

Surface Analysis. ATR-IR spectroscopy of an oxidized silicon prism functionalized with the ester, **5**, on one face only, shows a coverage of 50 ± 10 molecules nm^{-2}, which corresponds to a thickness of 26 nm and is about 20 times as thick as expected for a monolayer. The coverage was determined by comparison of the intensities of the ATR-IR signal of the ester group at 1738 cm^{-1} from the functionalized silicon surface with that of a clean silicon surface immersed in 0.1 M aqueous *N*-propyl-3,3′-iminodipropionic acid dimethyl ester (the methyl ester of **4**). The penetration depth of the evanescent wave into the aqueous solution was determined from the known optical properties of water. While the coverage on oxidized silicon and fused silica may not be identical, this result implies that the adsorbed film on fused silica is a multilayer, due to some degree of polymerization. Horizontal and vertical polymerization frequently occur when trimethoxysilanes adsorb onto silica, due to traces of moisture.[3,10] Vertical polymerization of **5**, via (CH$_2$)SiOSi(CH$_2$) links, increases the layer thickness but should not affect the surface functionality. AFM images of oxidized silicon functionalized with **5** (Supporting Information) show an undulating surface with an root-mean-square roughness of 2 nm, together with a significant number of randomly distributed approximately hemispherical particles with a typical size of 100 nm. This is in contrast to the same substrates prior to functionalization which show a root-mean-square roughness of 0.4 nm. Comparison with the mean film thickness of 26 nm determined by ATR-IR suggests that the uniform undulating part of the film has a thickness of about 20 nm, with roughly one-fifth of the absorbed material being present as larger aggregates. The increased roughness of the surface by functionalization does not significantly increase the surface area (<3%).

In situ ATR-IR was also used to monitor the hydrolysis of the surface ester groups, by observing the intensity of the C=O stretch; after 10 days the hydrolysis is >95% complete, and after 14 days no residual ester groups are detectable. Several other peaks, including those in the CH region (2900−3100 cm^{-1}) are unchanged during hydrolysis, which confirms that aqueous imidazole does not cleave the silane from the surface.

Films of disulfide **7** on gold were characterized by FTIR spectroscopy. From the intensity of the CH stretch band, we estimate[11,12] that the surface coverage is 2.3 ± 0.4 molecules nm^{-2}, which is consistent with a monolayer of a molecule with two tail groups.[13] FTIR spectra of gold treated with carbamate disulfide **8** show similar levels of surface coverage.

Dye Adsorption: Determining Surface Coverage. Dyes **1**−**3** were adsorbed onto the surfaces from aqueous solutions, to probe the charge-reversal properties of the surfaces. The copper(II) sulfonated porphyrin, **3**, was used, rather than the free base, to prevent protonation at the center of the macrocycle. The amount of dye adsorbed on the surface was determined by comparing the integral of the UV−vis. absorption band of the surface-bound dye with that of the same dye in solution at known concentration.[14] Raw spectra for porphyrin **2** in solution,

on functionalized fused silica, and on gold functionalized with **7** are shown in Figure 1. All adsorption and desorption experiments were reproducible within experimental error. The values for surface coverage obtained in this way were corrected to account for the optical properties of the interfaces, by comparison of experimental and theoretically produced spectra.[12,15,16] The dye absorption spectra were modeled as Lorentz oscillators (two each for dyes **1** and **3** and one for dye **2**). The solvent and silica real refractive indices were modeled with Cauchy functions with zero for their imaginary parts. For the solution spectra, this was combined with the dye indices using a Bruggeman effective medium approximation to produce effective optical constants for the system.[12] The surface absorption data were fitted assuming a thin film of dye (film thickness <10 nm).

Adsorption Characteristics. Preliminary experiments were carried out to test the rate of dye adsorption. A series of functionalized fused silica samples were immersed in a solution of methylene blue **1** at pH 7 for varying lengths of time before analysis. Under these conditions the cationic dye adsorbs onto the anionic surface. The results displayed in Figure 2 show that the adsorption process reaches equilibrium with a half-life ($t_{1/2}$) of 6900 s. Similar results were obtained with the porphyrins **2** and **3**. Adsorption of dyes onto functionalized gold surfaces reachs equilibrium much more rapidly, as illustrated by the adsorption of porphyrin **2** onto gold functionalized with **7** (Figure 3, $t_{1/2}$ = 62 s).

(11) The CH stretch region of the FTIR spectrum of **7** on gold was analyzed[12] using the isotropic imaginary part for the refractive index (k_{iso}), obtained by averaging published values of k_x, k_y, and k_z for the CH$_2$ groups of behenic acid methyl ester (BAME, CH$_3$(CH$_2$)$_{20}$CO$_2$CH$_3$; Pelletier, I.; Bourque, H.; Buffeteau, T.; Blaudez, D.; Desbat, B.; Pézolet, M. *J. Phys. Chem. B* **2002**, *106*, 1968−1976). The real part of the refractive index, n, was generated from the values of k by numerical Kramers−Kronig transformation with n_∞ as 1.41. These parameters were used to determine the thickness of an isotropic BAME film that would have an integrated absorbance in the CH stretch region equal to that in the reflectance spectrum of **7**, on gold at the same angle of incidence. Assuming that the BAME monolayer from which the optical constants were derived (Flach, C. R.; Gericke, A.; Mendelsohn, R. *J. Phys. Chem. B* **1997**, *101*, 58−65) had a typical coverage of 5.0 molecules nm^{-2} (Small, D. M. *The physical chemistry of lipids*: *from alkanes to phospholipids*; Plenum Press: New York, 1986), we estimate an equivalent coverage of BAME of 2.3 ± 0.5 molecules nm^{-2}. If we assume that all the CH$_2$ groups in **7** have the same oscillator strength as the CH$_2$ groups in BAME (there are an equal number of CH$_2$ groups in BAME and **7**) and that they are isotropically distributed, the coverage of **7** will also be 2.3 ± 0.4 molecules nm^{-2}.
(12) Film Wizard, 6.5.1 Scientific Computing International, 1999.
(13) Surprisingly, the CH$_2$ frequencies observed in films of **7** on gold (2849 and 2919 cm^{-1}) are typical of densely packed all-anti hydrocarbon chains. (Dubois, L. H.; Nuzzo, R. G. *Annu. Rev. Phys. Chem.* **1992**, *43*, 437−463.) If the layer is densely packed, it must be highly tilted to give the estimated area per molecule.
(14) McCallien, D. W. J.; Burn, P. L.; Anderson, H. L. *J. Chem. Soc., Perkin Trans. 1* **1997**, 2581−2586.
(15) A slight modification of the data was required before fitting to take into account the dye adsorbed onto both sides of the functionalized fused silica slides, because it is not possible to model a macroscopic layer (the 1 mm thick silica) with the software. Hence, the absorbance at each wavelength point in the spectra was halved, making the assumption that absorption and reflection at each air/silica interface contributes equally. The resulting transmission spectra were compared with those simulated for a single air/dye/functionalized silica interface. The data for absorption of dyes onto gold functionalized with **6** and **7** were normalized by reference to a protected aluminium mirror. The reflectivity data on gold were then fitted using the software material file for gold[12] and only varying the parameters of the dye thin film Lorentz functions. The simulation allows the absorbance of a free-standing film of dye to be calculated directly. Several sets of data at varying dye coverage for each dye were compared with simulated spectra, enabling correction factors to be calculated for the coverage obtained by direct integration of the spectra.
(16) The calculations assume a random orientation of the chromophores on the surfaces. If the dye molecules were aligned face-on (0° to the surface), then their absorptions relative to that of a randomly oriented configuration would be 150%. If they were aligned edge-on (90° to the surface), then their absorptions would be 75% for a dye of D_{4h} symmetry with two oscillators and 150% for methylene blue, **1**, with only one oscillator.

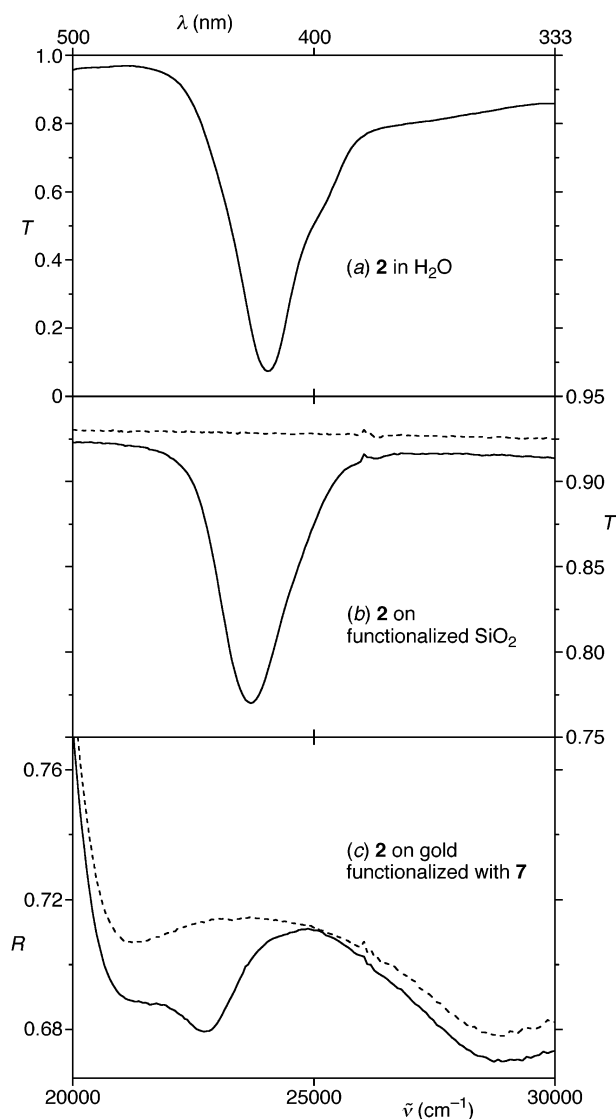(10) Fadeev, A. Y.; McCarthy, T. J. *Langmuir* **2000**, *16*, 7268−7274.

Figure 1. Representative transmittance (*T*) and reflectance (*R*) spectra of porphyrin **2** Soret band, (a) in water, 3.0 μM, (b) adsorbed on functionalized silica, and (c) adsorbed on gold functionalized with **7**. Dashed lines show background spectra for blank substrates.
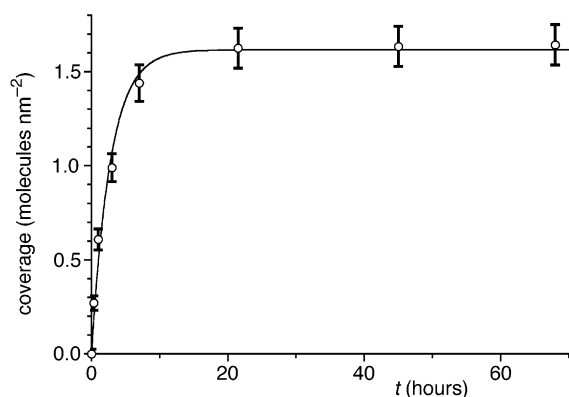

Figure 2. Time dependence of methylene blue, **1**, adsorption onto amphoteric functionalized fused silica, at pH 7, fitted to a first-order curve with $t_{1/2} = 6900$ s.

It is remarkable that equilibration on the gold surfaces is 2 orders of magnitude faster than that on functionalized silica. The structural origins of this kinetic difference have yet to be
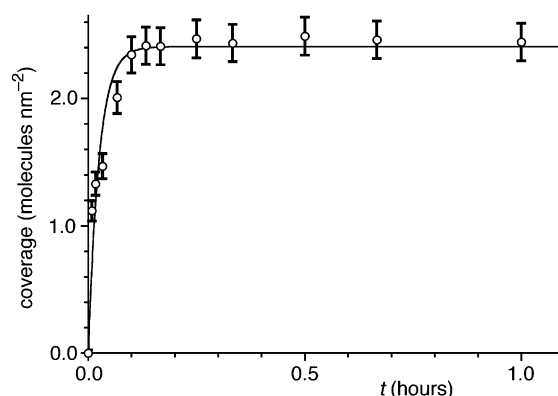

Figure 3. Time dependence of porphyrin **2** adsorption onto gold functionalized with disulfide **7**, at pH 1, fitted to a first-order curve with $t_{1/2} = 62$ s.

elucidated and may be associated with a slow release of countercations (e.g., Na$^+$) from the functionalized silica.

The surface coverages of each dye at pH 1 and 7 are listed in Table 1, together with calculated maximum coverages for close-packed monolayers.[17] Methylene blue molecules have an approximate face-on area of 1.1 ± 0.1 nm^2. Adsorption of methylene blue to mica gives a coverage of ca. 1.5 molecules nm^{-2}, with the molecules packing at an angle of 65−70° to the surface.[18] This is similar to the maximum coverage of 1.6 ± 0.1 molecules nm^{-2} for adsorption to our functionalized silica. The porphyrins, **2** and **3**, give similar maximum coverages to methylene blue, yet their calculated footprint areas are more than twice as large, implying that they must form multilayers to achieve these high surface densities.

The fixed incident angle of 6° to normal in our reflection equipment prevents us from obtaining good reflectance spectra of surface-bound methylene blue on gold, because the imaginary part of the refractive index is too high in this wavelength region (540−750 nm), resulting in a very high reflectivity and a node in the electric field at the interface. Fortunately, this is not a problem in the region of the porphyrin Soret band (370−460 nm). Comparison between adsorption of the porphyrins onto the functionalized silica and gold (Table 1) shows larger maximum adsorbances on the functionalized gold surfaces. The maximum charge density of **7** adsorbed on gold is 2.3 ± 0.5 charges nm^{-2} (assuming complete ionization of the carboxylates). Thus the observation that tetracationic porphyrin **2** adsorbs to a coverage of 2.3 ± 0.1 molecules nm^{-2} implies that some other interaction must augment electrostatic adsorption of the porphyrins onto this surface. Gold surfaces functionalized with the two disulfides, **6** and **7**, have similar levels of dye adsorption, as is to be expected if the adsorption is determined mainly by the amphoteric tail groups.

Variation in adsorption with pH: Demonstration of Charge Reversal. Surfaces were placed in dye solutions of varying pH; after 24 h each sample was removed, its UV−vis spectrum was recorded, and then the surface was reimmersed in a fresh dye solution of different pH. As the pH drops, the surface protonates and the charge is reversed. The affinity of

(17) Van der Waals footprint areas of molecules of dyes **1**−**3** were calculated using molecular mechanics (CaChe, 4.1, Oxford Molecular Ltd., 1999) and used to estimate monolayer coverages, assuming either flat or vertical orientations of the chromophores on the surface.

(18) Hähner, G.; Marti, A.; Spencer, N. D.; Caseri, W. R. *J. Chem. Phys.* **1996**, *104*, 7749−7757.

Table 1. Calculated and Observed Dye Coverage (molecules nm^{-2}) at pH 1 and pH 7[16]

	calcd monolayer coverage		coverage on silica functionalized with **5**		coverage on gold functionalized with **6**		coverage on gold functionalized with **7**	
dye	flat	vertical	pH 1	pH 7	pH 1	pH 7	pH 1	pH 7
1	0.9 ± 0.05	1.8 ± 0.09	0.02 ± 0.03	1.6 ± 0.1				
2	0.30 ± 0.02	0.84 ± 0.04	0.07 ± 0.03	1.8 ± 0.1	0.37 ± 0.04	2.2 ± 0.1	0.04 ± 0.03	2.3 ± 0.1
3	0.20 ± 0.01	0.57 ± 0.03	1.2 ± 0.09	0.19 ± 0.03	1.8 ± 0.1	0.20 ± 0.04	2.5 ± 0.2	0.14 ± 0.03
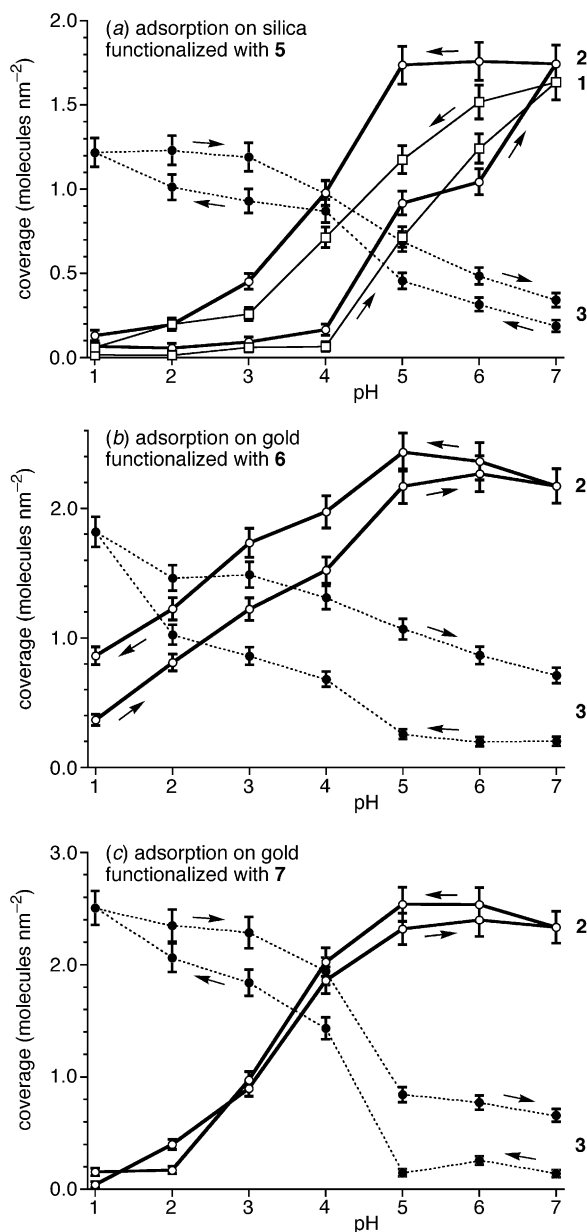
Figure 4. Adsorption of dyes **1** (□), **2** (○), and **3** (●) onto (a) fused silica functionalized with **5**, (b) gold functionalized with disulfide **6**, and (c) gold functionalized with disulfide **7**, as a function of pH. Arrows indicate the direction of pH increment.

the functionalized silica surface for positively charged dyes **1** and **2** increases with pH, while its affinity for negatively charged dye **3** decreases (Figure 4a). Similar behavior is seen for functionalized gold (Figure 4b,c). Gold functionalized with disulfide **7** shows a sharp charge reversal between pH 2 and pH 5, whereas the surface functionalized with disulfide **6** responds over a wider pH range. The level of adsorption does not drop to zero even when the charge on the surface should be
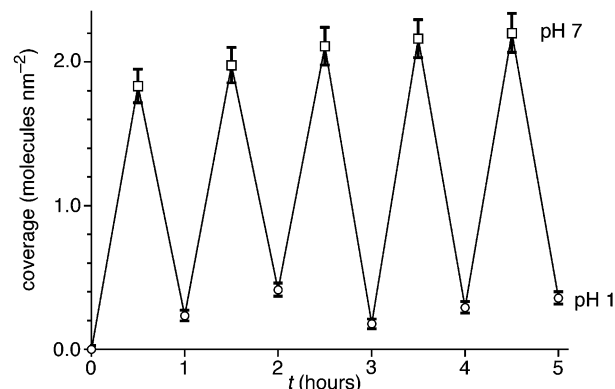
Figure 5. Sequential adsorption and desorption of porphyrin **2** to gold functionalized with disulfide **7**, by alternating (○) pH 1 and (□) pH 7.

the same as that of the dyes, revealing a low level of nonspecific binding. Control experiments were performed to test the adsorption of charged dyes to clean unfunctionalized substrates. The anionic dye **3** does not show any significant adsorption to silica at pH 1−7 (coverage <0.25 molecules nm^{-2}), whereas the cationic dyes **1** and **2** adsorb at pH 4−7, with coverages of up to 1.5 molecules nm^{-2}, as expected because clean silica has a negative surface charge in water at neutral pH ($pK_a \approx 4.3$).[19] Blank gold surfaces do not adsorb detectable levels of dyes **1**−**3**.

The similar maximum coverages of the anionic and cationic porphyrins, which are of comparable molecular sizes and charge densities, on all the amphoteric surfaces indicates that there is charge reversal on these surfaces across the pH range studied. The surface charge can be reversed repeatedly by switching the pH of the solution. Figure 5 shows a typical adsorption response to repeated switching of pH. The surface remains charge reversible through multiple cycles and thus has potential for reuse.

Irreversible Proton-Triggered Charge Switching. Gold functionalized with carbamate disulfide **8** was tested by adsorption of cationic and anionic porphyrins **2** and **3**, and the surface coverage was determined as described above. The kinetics of adsorption to gold surfaces functionalized with the three thiols **6**−**8** are essentially the same, with half-lives of about 1 min. In the pH range 2−7, no cleavage of the carbamate occurs (Figure 6a). The cationic porphyrin **2** adsorbs strongly at pH 7, when the surface carboxylates are ionized, and the coverage decreases reversibly with decreasing pH as the carboxylates protonate. As expected, the anionic porphyrin **3** does not adsorb strongly to this anionic surface. Solution NMR experiments show that carbamate **8** is rapidly cleaved by TFA (Scheme 2). Thus when gold surfaces functionalized with **8** are treated with hydrochloric acid (10 M), or TFA, there is an abrupt reversal in the adsorption characteristics as the surface functionality is transformed from

(19) Chaiyasut, C.; Takatsu, Y.; Kitagawa, S.; Tsuda, T. *Electrophoresis* **2001**, *22*, 1267−1272.
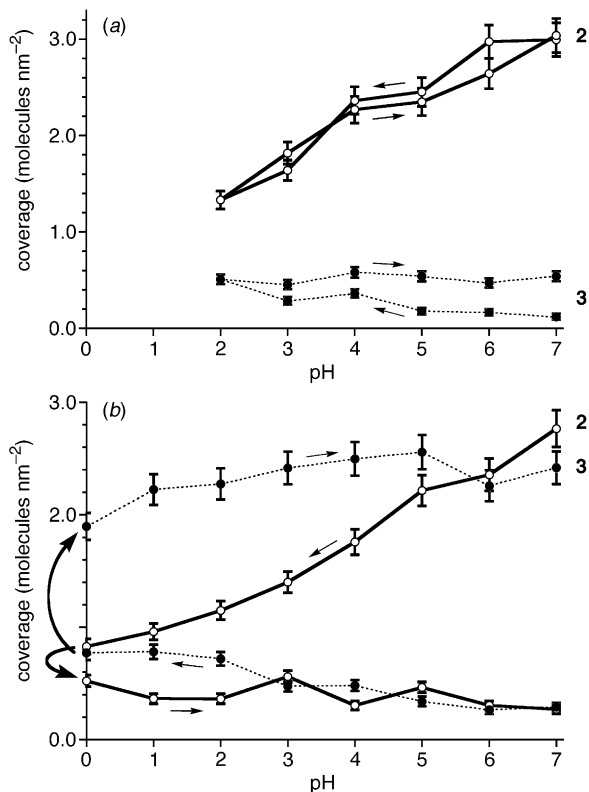
Figure 6. Adsorption of dyes **2** (○) and **3** (●) onto gold functionalized with carbamate-linked disulfide **8** as a function of pH (a) sweeping pH 7 → 2 → 7 (no irreversible charge switching) and (b) sweeping pH 7 → −1 → 7 (showing irreversible charge switching; see Scheme 2). Arrows indicate the direction of pH increment.

carboxylate to ammonium. In Figure 6b, the surface coverages were first monitored as the pH was scanned 7 → 0, and then the surface was briefly exposed to 10 M hydrochloric acid (pH ≈ −1), before remonitoring the adsorption as the pH was returned 0 → 7. Before acid treatment, the surface binds the cationic dye but not the anionic one; after acid treatment this selectivity is reversed, providing clear evidence for proton-triggered charge reversal.

Conclusions

We have created a range of surfaces which exhibit reversible, and irreversible, proton-induced charge reversal, as demonstrated by their changing affinity for positively and negatively charged dyes. The reversible surfaces are robust enough to allow their charge to be switched many times, whereas the irreversible surfaces undergo a single switch from anionic to cationic. These surfaces could be used as versatile control elements for the binding, manipulation and release of charged guests, such as dyes, pharmaceuticals, nanoparticles, or viruses.[1] Irreversible proton-triggered charge switching may also enable surfaces to be patterned by shadow-masked photoacid generation.[20]

Experimental Procedures

Preparation of Substrates. Fused silica microscope slides (15 × 15 × 1 mm from UQG Ltd.) were cleaned in 7:3 (v/v) H_2SO_4:30% H_2O_2 at 70 °C for 2 h **(Hazard: Corrosive! May react violently with organic matter!)** After cooling, the slides were rinsed with ultrapure water and dried in a stream of nitrogen. Gold surfaces were obtained

(20) Wallraff, G. M.; Hinsberg, W. D. *Chem. Rev.* **1999**, *99*, 1801−1821.

by vapor deposition of 5 nm of chromium followed by 200 nm of gold onto 16 × 16 mm² glass cut from microscope slides 1.2 mm thick and used fresh from the evaporator.

Substrate Functionalization. The fused silica slides were functionalized on both sides by heating at 80 °C for 4 h in a toluene solution of 10% (v/v) *N*-(trimethoxysilylpropyl)-3,3′-iminodipropionic acid dimethyl ester, **5**, with 0.1% (v/v) diisopropylethylamine.[13] The slides were rinsed in toluene, sonicated in fresh toluene for 30 s to remove physisorbed material, further rinsed in methanol, and then dried in a stream of nitrogen. These functionalized slides were then immersed in aqueous imidazole (2.6 M) for 14 days to achieve hydrolysis of the surface esters. The gold surfaces were functionalized by immersion for 1 h in a 0.1 mg/mL aqueous solution of disulfide, **6** or **7**, or 0.1 mg/mL **8** in DMSO, rinsed in ultrapure water to remove physisorbed material and dried in a stream of nitrogen. Newly functionalized substrates were used immediately to avoid accidental contamination.

Measurements of IR Spectra. Reflectance IR spectra of the monolayers on gold were measured with a Bio-Rad FTS6000 FTIR spectrometer, with a ceramic source, KBr beam splitter and linearized liquid nitrogen cooled MCT detector. Spectra were recorded at 60° with a Graseby Specac 19650 series variable angle accessory. ATR-IR spectra were also measured on this instrument using a Spectra-Tech Micro ATR prism holder, with a silicon prism, mounted in a Spectra-Tech beam condenser. A liquid cell was constructed, from stainless steel and Teflon, so that only one face of the silicon prism was exposed to the liquid during coating and analysis, while in the sample compartment of the spectrometer the other faces were open to the air, which was scrubbed to remove water, carbon dioxide, and hydrocarbons.

Dye Adsorption. As a means of probing the amphoteric nature of the surfaces, charged dyes were adsorbed from solutions with pH in the range of 1−7. The surfaces were immersed in 0.1 mg/mL aqueous solutions of both cationic and anionic dyes at an extreme of pH, either 1 or 7, for 24 h, removed and rinsed in ultrapure water for 10 s, dried in a stream of nitrogen, and then placed in the UV−vis spectrometer for analysis. The absorbance is measured, the surface is placed into a solution one pH increment on, and the process is repeated. All adsorption and desorption experiments were repeated more than once and produced consistent results within experimental error.

Measurements of Absorption and Reflection Spectra. Absorption spectra of chromophore layers adsorbed onto silica surfaces were measured with a Perkin-Elmer Lambda 20 UV−vis spectrometer. The samples were secured vertically so that the beam passed perpendicularly through the layers adsorbed on both sides of the slides. The absorption of the layers adsorbed onto gold surfaces was measured using a Perkin-Elmer specular reflectance accessory fitted into the beam path of the Perkin-Elmer Lambda 20 UV−vis spectrometer; a protected aluminum mirror was used to normalize the data. The beam was reflected off the gold surface at 6° to the normal. Since all the samples, both fused silica and gold, showed some background absorbance, spectra of the surfaces prior to dye adsorption were obtained for each sample and subtracted from subsequent spectra.

Supporting Information Available: Synthetic schemes and experimental procedures for preparation of compounds **5**−**8**, examples of ATR-IR and FTIR spectra, adsorption of dyes **1** and **3** onto clean silica as a function of pH, details of AFM measurements, and ¹³C and ¹H NMR spectra of **10**, **12**, **14**, and **17**. This material is available free of charge via the Internet at http://pubs.acs.org.

JA028338B